Computational Magnetic Resonance Imaging Based on Bloch NMR Flow Equation and Bessel Functions

O.B. Awojoyogbe* O.M. Dada and O.A. Adesola

Department of Physics, Federal University of Technology,
P.M.B. 65, Minna, Niger State, Nigeria

*E-mail: awojoyogbe@yahoo.com

Abstract. Detailed understanding of the complexities of flow and in biological materials is essential for the design, development, and optimization of MRI protocols for medical and biomedical applications. However, the design of such processes resort to trial and error, because the mathematics and physics of most experimental techniques are fundamentally limited. In this study, we develop a new magnetic resonance imaging sequence based on Bloch NMR flow equation and Bessel functions for detailed computational and experimental studies to improve health care.

Keywords: Bloch NMR flow equation, Bessel functions, Computational MRI.

1 Introduction

In Magnetic resonance imaging (MRI), an atomic nucleus resonates if exposed to a static magnetic field, when a varying electromagnetic field is applied at the proper frequency [1, 2]. An Image is computed from the resonance signals of which the frequency and phase (timing) contain spatial information. MRI is important because it is noninvasive, safe, and yields information that cannot be obtained with any other techniques. Its most common use by far is in diagnostic medicine but MRI has other applications, particularly in the oil and food industries [1, 2].

Since the nuclei from different regions of the body can be made to precess at different frequencies (their magneto-resonance frequencies), the electromagnetic energy at these frequencies yields signals that are location – dependent. Computer images can be calculated, enhanced, and displayed. MRI is safe because only a very tiny amount of energy is absorbed or emitted, corresponding to the amount of energy in radio waves, to which humans are constantly exposed. MRI does not affect any chemical processes. It does not change molecules at all. The atomic nuclei within the molecules just report what is happening.

In the static magnetic field, B_0 the nuclei are primed for a response to a transient magnetic field B_1 at their resonance frequency which changes their energy status. When the transient field is switched off, the nuclei emit radio waves as they return to their steady state condition. These re-radiated signals yield NMR spectra or MR images. Many different atomic nuclei (those that possess a net nuclear spin) are susceptible to NMR, and a few produce signals that are strong enough for diagnostic MRI. The nucleus of the hydrogen atom (a single proton) has the largest gyromagnetic ratio and has the highest energy and therefore the largest signal at any given field strength. Hydrogen is abundant as an element of water [2]. *The human body is about two thirds water*, so the combination of natural abundance and signal strength determines that imaging with the hydrogen nucleus gives the highest possible resolution. Nearly all clinical MRI is proton or hydrogen MRI. Other nuclei such as ^{23}Na and ^{31}P are also used, although until now primarily in research [2]. For MRI, as opposed to NMR, spatial gradients of magnetic field (G) are also needed. The gradient G makes the field experienced by each nucleus dependent upon its location within an object. For example G_x is a linear gradient along the x-axis and produces an extra field [2]:

$$G_x \mathrm{x} \tag{1}$$

at the point of x. Together G_x, G_y and G_z determine a unique point (x, y, z) in three-dimensional space.

New MRI methods are invented regularly, each having different advantages and disadvantages, depending on the type of image desired. While recent and current

practices of MRI in medicine have used techniques to acquire two-dimensional images, in principle and increasingly in practice, the methodology can be extended to three-dimensions or more, the only limitation being the amount of resonance signal that can be acquired and the capability of the hardware and software used for image formation [2]. MRI techniques are still evolving rapidly, as they are optimized for specific applications.

In this contribution, we have developed the analytical solutions of the Bloch NMR equation [3 – 6] into Bessel differential equation in terms of all relevant NMR/MRI flow parameters. The solutions of the Bessel equation in terms of the MRI parameters make this method unique and significantly useful for computational and experimental studies of NMR/MRI for resolving the difficulties usually encountered in previous and current MRI studies [3 – 6].

2 Theoretical Formulation

We study the flow properties of the modified time independent Bloch NMR flow equations which describe the dynamics of fluid flow under the influence of RF magnetic field as derived in the earlier studies [3 – 6].

$$v^2 \frac{d^2 M_y}{dx^2} + v\left(\frac{1}{T_1} + \frac{1}{T_2}\right)\frac{dM_y}{dx} + \left(\gamma^2 B_1^2(x) + \frac{1}{T_1 T_2}\right)M_y = \frac{M_o \gamma B_1(x)}{T_1} \qquad (2)$$

Subject to the following conditions:

(i) $M_o \neq M_z$ a situation which holds good in general and in particular when the RF $B_1(x)$ field is strong say of the order of 1.0G or more.

(ii) before entering signal detector coil, fluid particles has magnetization $M_x = 0$, $M_y = 0$.

(iii) if $B_1(x)$ is large; $B_1(x) >> 1G$ or more so that M_y of the fluid bolus changes appreciably from M_o. For this investigation, we assumed that the resonance condition existed at Larmor frequency: $f_0 = \gamma B - \omega = 0$

(iv) for steady flow, $\frac{\partial M_y}{\partial t} = 0$.

γ denotes the gyromagnetic ratio of fluid spins; $\omega/2\pi$ is the RF excitation frequency; f_o/γ is the off- resonance field in the rotating frame of reference.T_1 and T_2 are the spin-lattice and spin-spin relaxation times respectively, the reciprocals of T_1 and T_2 are defined as relaxation rates. v is the fluid flow velocity and RF $B_1(x)$ is the spatially varying magnetic field defined as: $\gamma B_1(x) = \gamma G x$ (3)

In a typical MRI procedure, G is the pulsed gradient applied for the length of time t. Substituting for equation (3) in (2) gives:

$$x^2 \frac{d^2 M_y}{dx^2} + x\alpha \frac{dM_y}{dx} + \left(\left(\gamma \frac{\alpha}{T_o} G \right)^2 x^2 + \frac{\alpha^2}{T_1 T_2} \right) M_y = \frac{M_o \gamma B_1(x)}{T_1} \quad (4)$$

Maximum signal is expected when RF $B_1(x)$ has the largest magnitude so that the equilibrium magnetization M_o is very small (say $M_o \approx 0$). Hence, for maximum value of M_y, we can write equation (4) as:

$$x^2 \frac{d^2 M_y}{dx^2} + x\alpha \frac{dM_y}{dx} + \left(\left(\gamma \frac{\alpha}{T_o} G \right)^2 x^2 + \frac{1}{T_1 T_2} \left(\frac{\alpha}{T_o} \right)^2 \right) M_y = 0 \quad (5a)$$

$$x^2 \frac{d^2 M_y}{dx^2} + x\alpha \frac{dM_y}{dx} + \left((\theta)^2 x^2 + \frac{\tau^2}{T_1 T_2} \right) M_y = 0 \quad (5b)$$

where $x = \frac{\alpha v}{T_o} = vnTR = v\tau$ (6a)

where n is the number of pulses, TR is the repetion time, τ is the time between two pulses and

$$n = \frac{T_o TR}{\alpha} \quad (6b)$$

$$\tau = nTR \quad (6c)$$

Equation (5) is a general form of an equation transformable into Bessel equation of order β with parameter k. A general solution of equation (5a) is in the form [7, 8]:

$$M_y(x) = x^{-p} \left[c_1 J_n(\beta x) + c_2 Y_n(\beta x) \right] \quad (6d)$$

where p, n, β are all constants defined as [7]:

$$n = \frac{\sqrt{(2p)^2 - 4T_g(\alpha/T_0)^2}}{2} = \sqrt{p^2 - T_g(\alpha/T_0)^2} \tag{7a}$$

$$\theta = \gamma G\left(\frac{\alpha}{T_0}\right) = \gamma G\tau \tag{7b}$$

$$\alpha = 1 - 2p \tag{7c}$$

$$T_0 = \left(\frac{1}{T_1} + \frac{1}{T_2}\right) = \frac{(T_1 + T_2)}{T_1 T_2} \tag{8a}$$

$$T_g = \frac{1}{T_1 T_2} \tag{8b}$$

$$\beta = \sqrt{T_g}(\alpha/T_0) = \tau\sqrt{T_g} \tag{8c}$$

Since the transverse magnetization needs to have a finite limit as x tends to zero, $c_2 = 0$ [7, 8] and

$$M_y(x) = c_1 x^{-p} J_\beta(\theta x) \tag{9}$$

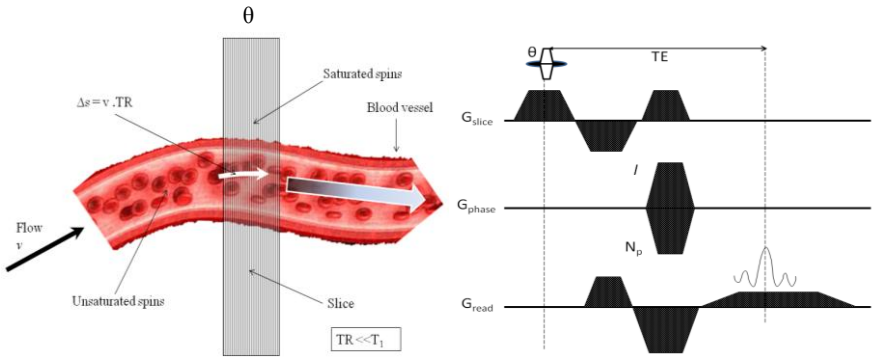

Fig. 1. Illustration of the flip angle $\theta(rad) = \gamma(rad \ \ \sec^{-1} \ G^{-1})(G)\tau(\sec)$ [t = τ = $\frac{\alpha}{T_o}$ in equation (5)] and the corresponding MRI sequence.

In equation (5) and (9), τ is defined as the time between pulses in the experiment, c_1 is the initial amplitude of the transverse magnetization M_y, and the observed signal voltage is directly proportional to M_y. Equation (5) and (9) are new ways of generating the NMR signal using the Bessel functions. As shown in figure 1, the experiment is started with a 90^o pulse, following which the magnetic vector M_y precesses in the plane perpendicular to the direction of static magnetic field B_o, and free induction decay (FID) occurs. The maximum amplitude of the FID is measured to obtain a voltage-amplitude fiducial mark for c_1. After a delay which is typically of the order of 10ms [9], a 180^o RF pulse is introduced. Following another interval τ, the magnetic spins re cluster and a spin echo voltage signal is observed. The voltage amplitude of the spin echo is taken as proportional to M_y in equation (9) and equation (5) is then solved for β. To solve equation (5), the value of G must be known, as well as the gyromagnetic ratio γ of the specific nuclei under study. Both constants are easily at hand, G is measured independently and γ may be found in a tabulation of atomic constants. The voltage amplitude of the spin echo M_y is easily computed by solving the Bessel equation (equation (5)) of order β and parameter θ.

3 Analysis of Results

Tables (1-9) and figures (2-11) are developed based on the following parameters: $\gamma = 4.25716 \times 10^7$ Hz.T^{-1} and G = 0.2Tm^{-1} [1, 9].

Tissues	T_1(s)	T_2(s)	T_g(s^{-2})	T_0(s^{-1})	$\frac{T_g}{T_0^2}$	$\frac{\gamma G}{T_0}$
Skeletal muscle	1.03	0.060	16.18123	17.63754	0.052015824	482738.5101
Heart muscle	1.01	0.073	13.56300	14.68873	0.062861874	579649.8741
Liver	0.61	0.057	28.76043	19.18320	0.078154326	443842.4384
Kidney	0.83	0.082	14.69292	13.39994	0.081828062	635399.8018
Spleen	0.93	0.089	12.08167	12.31122	0.079712162	691590.0553
Fatty tissue	0.330	0.120	25.25253	11.36364	0.195555556	749260.1600
Gray brain matter	1.08	0.124	7.467145	8.990442	0.092383086	947041.3076
White brain matter	0.92	0.114	9.534706	9.858886	0.098096068	863618.8410

Table 1. Relaxation parameters for different tissues and relaxation rates at 1.5T [1].

x(m)	T_2(s)	T_1(s)	T_g(s^{-2})	T_0(s^{-1})	v(ms^{-1})	α/T_0	n	β	M_y(x)
0.00	0.0290	0.390	88.41733	37.04686	0	0.404893	5.874099	3447385	0
0.01	0.0318	0.412	76.32656	33.87373	0.022582	0.442821	5.833788	3770320	-6796.94
0.02	0.0346	0.434	66.59386	31.20588	0.041608	0.480679	5.797703	4092652	3315369
0.03	0.0374	0.456	58.63589	28.93095	0.057862	0.518476	5.765211	4414470	24511236
0.04	0.0402	0.478	52.04105	26.96767	0.071914	0.556222	5.735801	4735848	2.95E+08
0.05	0.0430	0.500	46.51163	25.25581	0.084186	0.593923	5.709054	5056848	-8.6E+07
0.06	0.0458	0.522	41.82770	23.74977	0.094999	0.631585	5.684623	5377517	2.64E+09
0.07	0.0486	0.544	37.82377	22.41437	0.104600	0.669214	5.662221	5697899	1.01E+10
0.08	0.0514	0.566	34.37324	21.22204	0.113184	0.706812	5.641603	6018027	-2.4E+10
0.09	0.0542	0.588	31.37786	20.15086	0.120905	0.744385	5.622566	6337931	1.74E+10
0.10	0.0570	0.610	28.76043	19.18320	0.127888	0.781934	5.604933	6657637	2.90E+10

Table 2. Relaxation parameters and the corresponding transverse magnetization of human liver at 1.5T [1]. The relaxations times are mapped to locations x within the range 0 to 0.1m, $c_1 = 1 \times 10^{21}$.

x(m)	T_2(s)	T_1(s)	$T_g(s^{-2})$	$T_0(s^{-1})$	$v(ms^{-1})$	α/T_0	n	β	$M_y(x)$
0.000	0.0290	0.390	88.41733	37.04686	0	0.404893	5.874099	3447385	0
0.001	0.0318	0.412	76.32656	33.87373	0.002258	0.442821	5.833788	3770320	-0.00473
0.002	0.0346	0.434	66.59386	31.20588	0.004161	0.480679	5.797703	4092652	-0.70133
0.003	0.0374	0.456	58.63589	28.93095	0.005786	0.518476	5.765211	4414470	-10.9951
0.004	0.0402	0.478	52.04105	26.96767	0.007191	0.556222	5.735801	4735848	-88.3813
0.005	0.0430	0.500	46.51163	25.25581	0.008419	0.593923	5.709054	5056848	-33.2875
0.006	0.0458	0.522	41.8277	23.74977	0.009500	0.631585	5.684623	5377517	201.2298
0.007	0.0486	0.544	37.82377	22.41437	0.010460	0.669214	5.662221	5697899	-3006.07
0.008	0.0514	0.566	34.37324	21.22204	0.011318	0.706812	5.641603	6018027	7590.508
0.009	0.0542	0.588	31.37786	20.15086	0.012091	0.744385	5.622566	6337931	15395.43
0.01	0.0570	0.610	28.76043	19.1832	0.012789	0.781934	5.604933	6657637	-26838.1

Table 3. Relaxation parameters and the corresponding transverse magnetization of human liver at 1.5T [1]. The relaxations times are mapped to locations x within the range 0 to 0.01m, $c_1 = 1 \times 10^{21}$.

x(m)	T_2(s)	T_1(s)	$T_g(s^{-2})$	$T_0(s^{-1})$	$v(ms^{-1})$	α/T_0	n	β	$M_y(x)$
0	0.029	0.39	88.41733	37.04686	0	0.404893	5.874099	3447385	0
0.000001	0.0318	0.412	76.32656	33.87373	2.26E-06	0.442821	5.833788	3770320	1.07E-22
0.000002	0.0346	0.434	66.59386	31.20588	4.16E-06	0.480679	5.797703	4092652	1.84E-20
0.000003	0.0374	0.456	58.63589	28.93095	5.79E-06	0.518476	5.765211	4414470	3.69E-19
0.000004	0.0402	0.478	52.04105	26.96767	7.19E-06	0.556222	5.735801	4735848	-1.1E-19
0.000005	0.043	0.500	46.51163	25.25581	8.42E-06	0.593923	5.709054	5056848	-1.8E-18
0.000006	0.0458	0.522	41.8277	23.74977	9.50E-06	0.631585	5.684623	5377517	1.71E-17
0.000007	0.0486	0.544	37.82377	22.41437	1.05E-05	0.669214	5.662221	5697899	1.03E-16
0.000008	0.0514	0.566	34.37324	21.22204	1.13E-05	0.706812	5.641603	6018027	-1.1E-16
0.000009	0.0542	0.588	31.37786	20.15086	1.21E-05	0.744385	5.622566	6337931	-3.8E-17
0.000010	0.057	0.61	28.76043	19.1832	1.28E-05	0.781934	5.604933	6657637	-3.4E-18

Table 4. Relaxation parameters and the corresponding transverse magnetization of human liver at 1.5T 1]. The relaxations times are mapped to locations x within the range 0 to 10×10^{-6}m, $c_1 = 1 \times 10^{21}$.

x(m)	T_2(s)	T_1(s)	$T_g(s^{-2})$	$T_0(s^{-1})$	$v(ms^{-1})$	α/T_0	n	β	$M_y(x)$
0	0.029	0.390	88.41733	37.04686	0	0.404893	5.874099	3447385	0
1E-09	0.0318	0.412	76.32656	33.87373	2.26E-09	0.442821	5.833788	3770320	1.98E-58
2E-09	0.0346	0.434	66.59386	31.20588	4.16E-09	0.480679	5.797703	4092652	1.22E-54
3E-09	0.0374	0.456	58.63589	28.93095	5.79E-09	0.518476	5.765211	4414470	2.32E-52
4E-09	0.0402	0.478	52.04105	26.96767	7.19E-09	0.556222	5.735801	4735848	1.04E-50
5E-09	0.0430	0.500	46.51163	25.25581	8.42E-09	0.593923	5.709054	5056848	2.10E-49
6E-09	0.0458	0.522	41.82770	23.74977	9.50E-09	0.631585	5.684623	5377517	2.55E-48
7E-09	0.0486	0.544	37.82377	22.41437	1.05E-08	0.669214	5.662221	5697899	2.16E-47
8E-09	0.0514	0.566	34.37324	21.22204	1.13E-08	0.706812	5.641603	6018027	1.41E-46
9E-09	0.0542	0.588	31.37786	20.15086	1.21E-08	0.744385	5.622566	6337931	7.52E-46
1E-08	0.0570	0.610	28.76043	19.1832	1.28E-08	0.781934	5.604933	6657637	3.41E-45

Table 5. Relaxation parameters and the corresponding transverse magnetization of human liver at 1.5T [1]. The relaxations times are mapped to locations x within the range 0 to 10×10^{-9}m, $c_1 = 1 \times 10^{21}$.

x(m)	T_2(s)	T_1(s)	$T_g(s^{-2})$	$T_0(s^{-1})$	$v(ms^{-1})$	α/T_0	n	β	$M_y(x)$
0	0.034	0.47	62.57822	31.53942	0	0.475595	5.902998	4049370	0
0.01	0.0388	0.506	50.93517	27.74948	0.0185	0.540551	5.840976	4602421	-29236.6
0.02	0.0436	0.542	42.31694	24.7808	0.033041	0.605307	5.787504	5153781	-2339039
0.03	0.0484	0.578	35.74595	22.39126	0.044783	0.669904	5.740926	5703779	21934726
0.04	0.0532	0.614	30.61399	20.42566	0.054468	0.734371	5.699989	6252665	-1.3E+08
0.05	0.058	0.65	26.5252	18.77984	0.062599	0.798729	5.663725	6800633	-5.8E+08
0.06	0.0628	0.686	23.2122	17.38129	0.069525	0.862997	5.631377	7347831	1.85E+08
0.07	0.0676	0.722	20.48878	16.17794	0.075497	0.927188	5.602342	7894379	-3.4E+09
0.08	0.0724	0.758	18.22184	15.13142	0.080701	0.991315	5.576136	8440373	5.87E+09
0.09	0.0772	0.794	16.31407	14.21281	0.085277	1.055386	5.552365	8985891	4.13E+10
0.10	0.082	0.83	14.69292	13.39994	0.089333	1.119408	5.530704	9530997	4.64E+10

Table 6. Relaxation parameters and the corresponding transverse magnetization of human kidney at 1.5T [1]. The relaxations times are mapped to locations x within the range 0 to 0.1m, $c_1 = 1 \times 10^{21}$.

x(m)	T_2(s)	T_1(s)	$T_g(s^{-2})$	$T_0(s^{-1})$	$v(ms^{-1})$	α/T_0	n	β	$M_y(x)$
0.000	0.034	0.47	62.57822	31.53942	0	0.475595	5.902998	4049370	0
0.001	0.0388	0.506	50.93517	27.74948	0.00185	0.540551	5.840976	4602421	0.008393
0.002	0.0436	0.542	42.31694	24.7808	0.003304	0.605307	5.787504	5153781	0.713355
0.003	0.0484	0.578	35.74595	22.39126	0.004478	0.669904	5.740926	5703779	13.22279
0.004	0.0532	0.614	30.61399	20.42566	0.005447	0.734371	5.699989	6252665	27.73395
0.005	0.058	0.65	26.5252	18.77984	0.00626	0.798729	5.663725	6800633	-269.199
0.006	0.0628	0.686	23.2122	17.38129	0.006953	0.862997	5.631377	7347831	-242.925
0.007	0.0676	0.722	20.48878	16.17794	0.00755	0.927188	5.602342	7894379	-1896.76
0.008	0.0724	0.758	18.22184	15.13142	0.00807	0.991315	5.576136	8440373	316.0689
0.009	0.0772	0.794	16.31407	14.21281	0.008528	1.055386	5.552365	8985891	13119.35
0.01	0.082	0.83	14.69292	13.39994	0.008933	1.119408	5.530704	9530997	-11309.7

Table 7. Relaxation parameters and the corresponding transverse magnetization of human kidney at 1.5T [1] The relaxations times are mapped to locations x within the range 0 to 10×10^{-3}m, $c_1 = 1 \times 10^{21}$.

x(m)	T_2(s)	T_1(s)	$T_g(s^{-2})$	$T_0(s^{-1})$	$v(ms^{-1})$	α/T_0	n	β	$M_y(x)$
0	0.0340	0.47	62.57822	31.53942	0	0.475595	5.902998	4049370	0
0.000001	0.0388	0.506	50.93517	27.74948	1.85E-06	0.540551	5.840976	4602421	2.08E-22
0.000002	0.0436	0.542	42.31694	24.7808	3.3E-06	0.605307	5.787504	5153781	-3.3E-20
0.000003	0.0484	0.578	35.74595	22.39126	4.48E-06	0.669904	5.740926	5703779	-4.2E-19
0.000004	0.0532	0.614	30.61399	20.42566	5.45E-06	0.734371	5.699989	6252665	-1.1E-18
0.000005	0.058	0.65	26.5252	18.77984	6.26E-06	0.798729	5.663725	6800633	8.9E-18
0.000006	0.0628	0.686	23.2122	17.38129	6.95E-06	0.862997	5.631377	7347831	-1.3E-17
0.000007	0.0676	0.722	20.48878	16.17794	7.55E-06	0.927188	5.602342	7894379	-8.5E-17
0.000008	0.0724	0.758	18.22184	15.13142	8.07E-06	0.991315	5.576136	8440373	-1.7E-16
0.000009	0.0772	0.794	16.31407	14.21281	8.53E-06	1.055386	5.552365	8985891	-4.2E-16
0.000010	0.082	0.83	14.69292	13.39994	8.93E-06	1.119408	5.530704	9530997	3.23E-16

Table 8. Relaxation parameters and the corresponding transverse magnetization of human kidney at 1.5T [1]. The relaxations times are mapped to locations x within the range 0 to 10×10^{-6}m, $c_1 = 1 \times 10^{21}$.

x(m)	T_2(s)	T_1(s)	$T_g(s^{-2})$	$T_0(s^{-1})$	$v(ms^{-1})$	α/T_0	n	β	$M_y(x)$
0	0.034	0.470	62.57822	31.53942	0	0.475595	5.902998	4049370	0
1E-09	0.0388	0.506	50.93517	27.74948	1.85E-09	0.540551	5.840976	4602421	5.38E-58
2E-09	0.0436	0.542	42.31694	24.7808	3.3E-09	0.605307	5.787504	5153781	3.88E-54
3E-09	0.0484	0.578	35.74595	22.39126	4.48E-09	0.669904	5.740926	5703779	8.35E-52
4E-09	0.0532	0.614	30.61399	20.42566	5.45E-09	0.734371	5.699989	6252665	4.18E-50
5E-09	0.058	0.650	26.5252	18.77984	6.26E-09	0.798729	5.663725	6800633	9.25E-49
6E-09	0.0628	0.686	23.2122	17.38129	6.95E-09	0.862997	5.631377	7347831	1.21E-47
7E-09	0.0676	0.722	20.48878	16.17794	7.55E-09	0.927188	5.602342	7894379	1.11E-46
8E-09	0.0724	0.758	18.22184	15.13142	8.07E-09	0.991315	5.576136	8440373	7.66E-46
9E-09	0.0772	0.794	16.31407	14.21281	8.53E-09	1.055386	5.552365	8985891	4.31E-45
1E-08	0.082	0.830	14.69292	13.39994	8.93E-09	1.119408	5.530704	9530997	2.05E-44

Table 9. Relaxation parameters and the corresponding transverse magnetization of human kidney at 1.5T. The relaxations times are mapped to locations x within the range 0 to 10×10^{-9}m, $c_1 = 1 \times 10^{21}$[1].

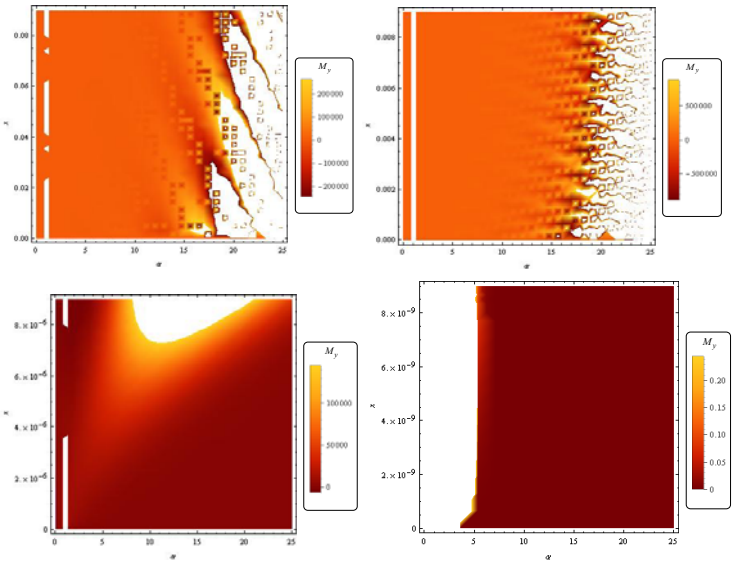

Fig. 2. Density plots of transverse magnetization as a function of location, x (at different value ranges) and α for skeletal muscle at 1.5Tbased on table 1.

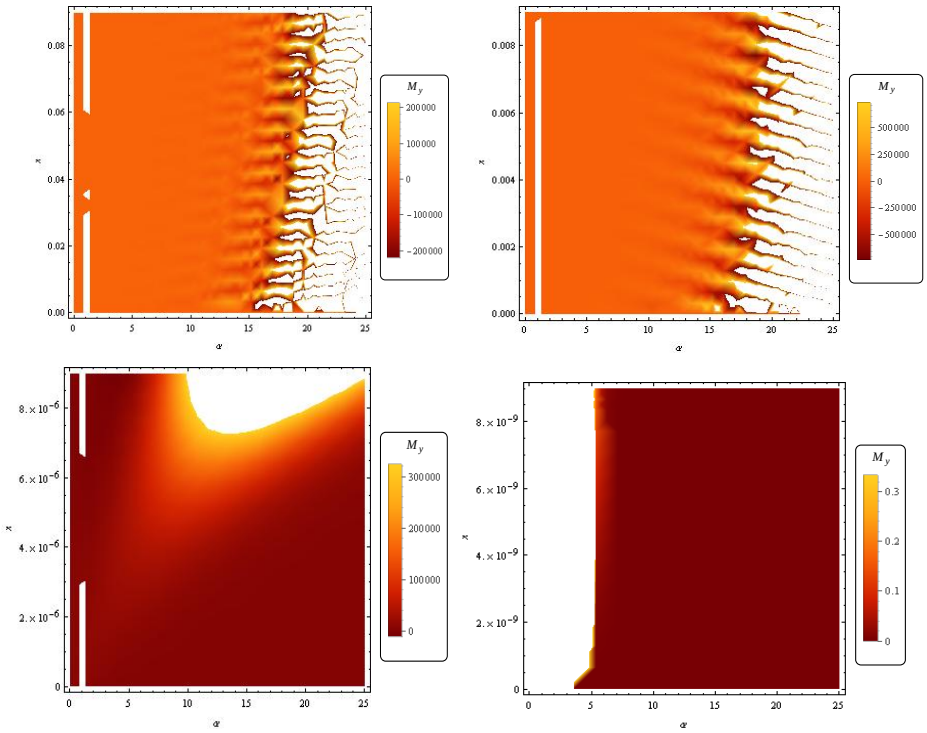

Fig. 3. Density plots of transverse magnetization as a function of location, x (at different value ranges) and α for heart muscle at 1.5T based on table 1.

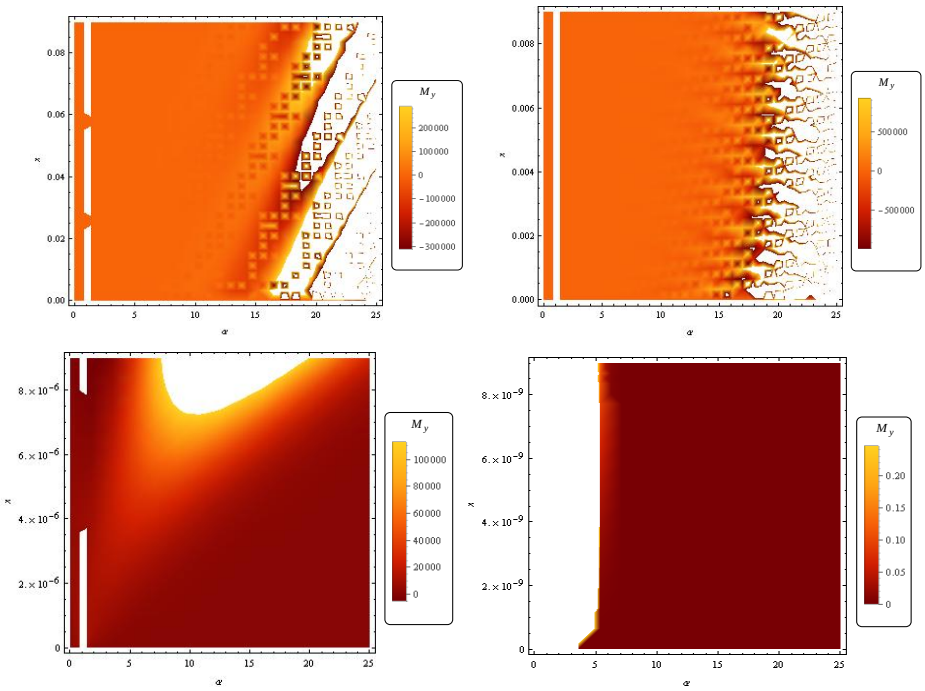

Fig. 4. Density plots of transverse magnetization as a function of location, x (at different value ranges) and α for liver at 1.5T based on table 1.

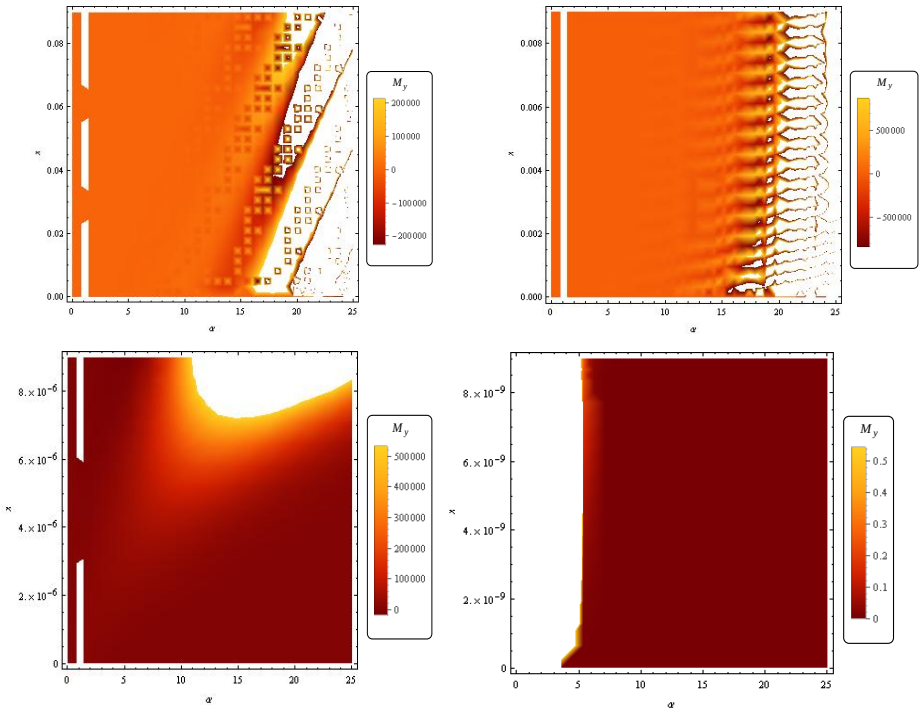

Fig. 5. Density plots of transverse magnetization as a function of location, x (at different value ranges) and α for kidney at 1.5T based on table 1.

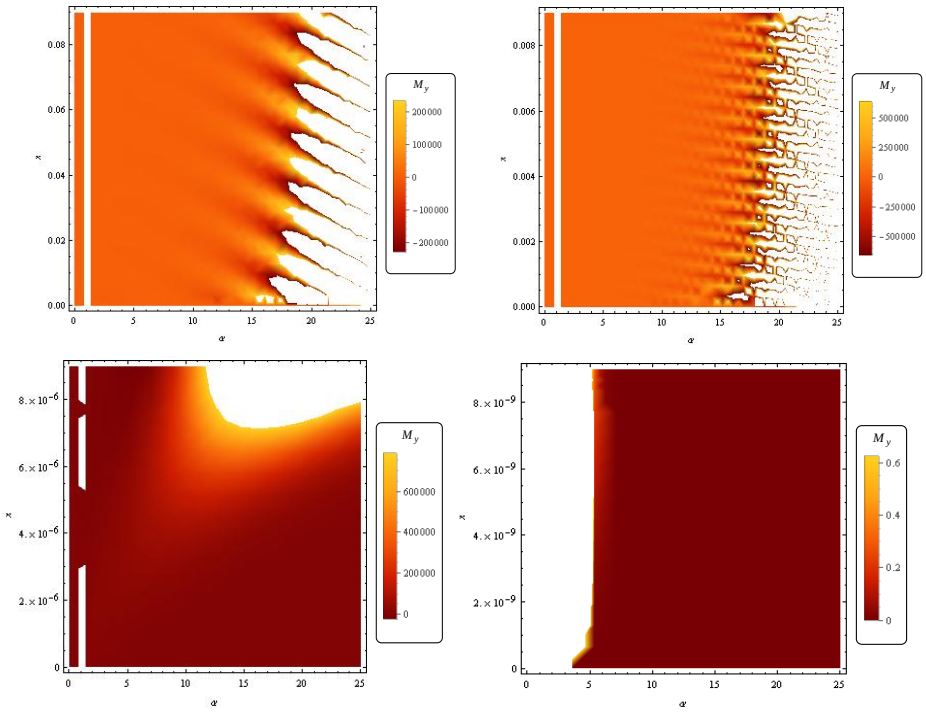

Fig. 6. Density plots of transverse magnetization as a function of location, x (at different value ranges) and α for spleen at 1.5T based on table 1.

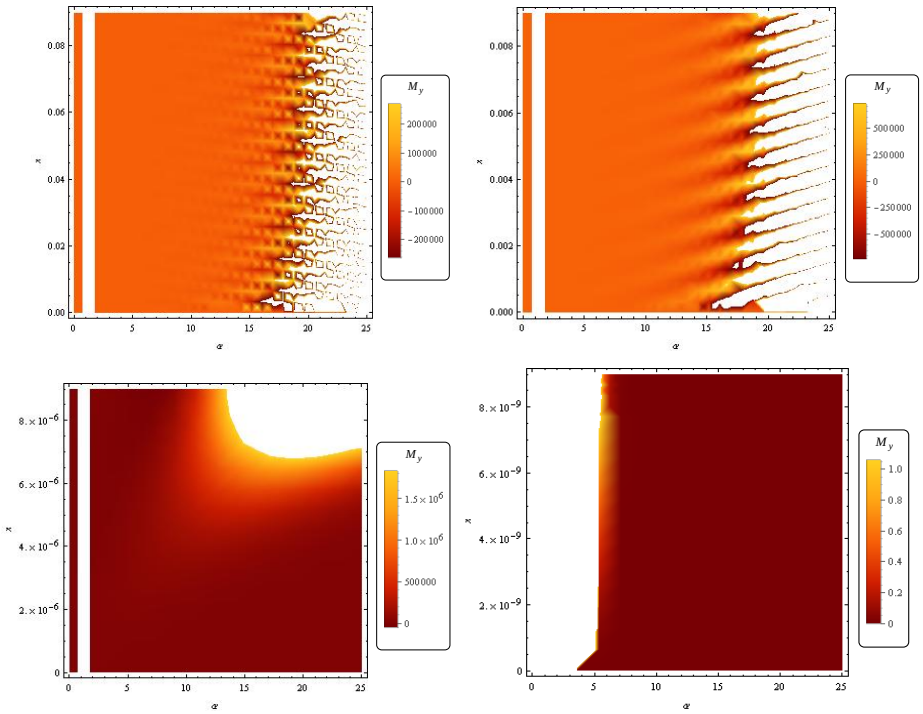

Fig. 7. Density plots of transverse magnetization as a function of location, x (at different value ranges) and α for fatty tissue at 1.5T based on table 1.

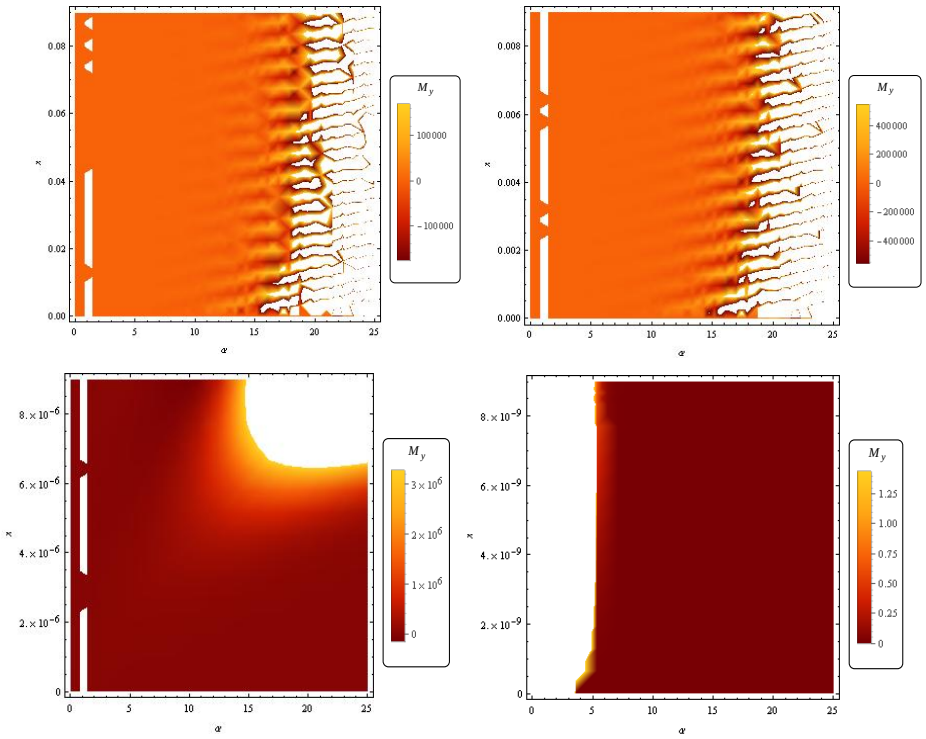

Fig. 8. Density plots of transverse magnetization as a function of location, x (at different value ranges) and α for Grey brain matter at 1.5T based on table 1.

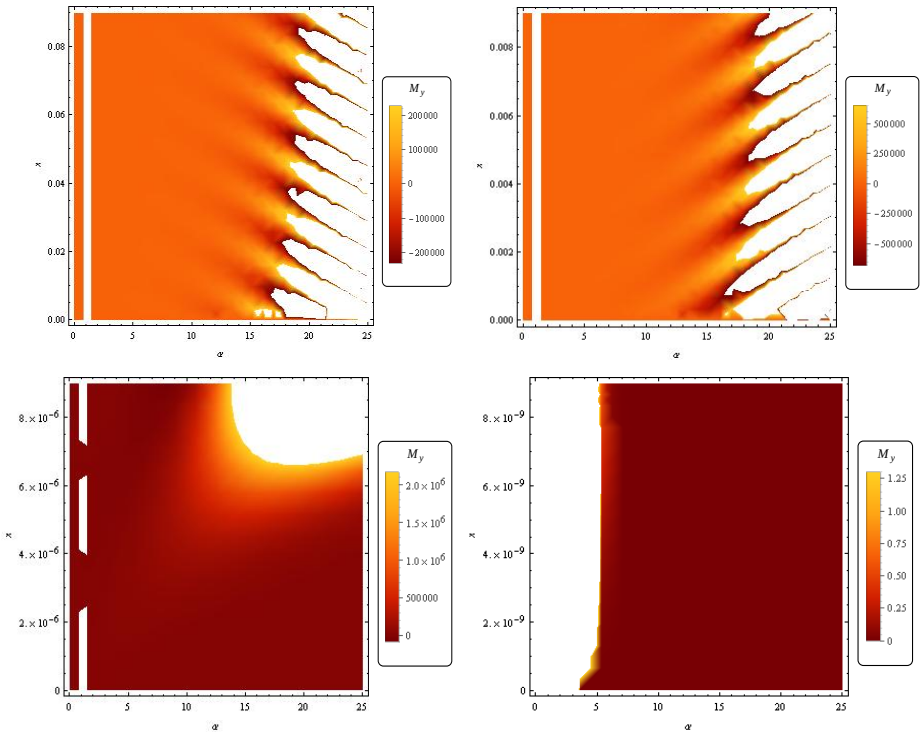

Fig. 9. Density plots of transverse magnetization as a function of location, x (at different value ranges) and α for White brain matter at 1.5T based on table 1.

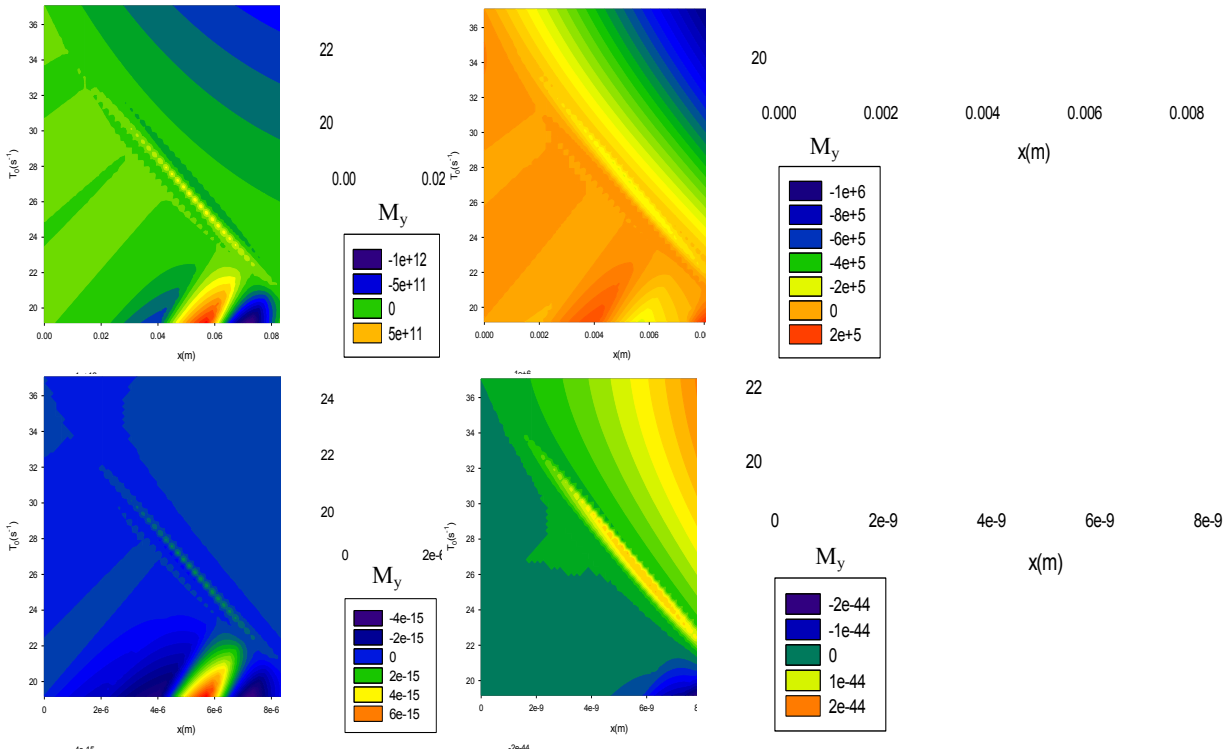

Fig. 10. Density maps of transverse magnetization as a function of location, x (at different value ranges) and T_0 for liver at 1.5T ased on tables 2 - 5.

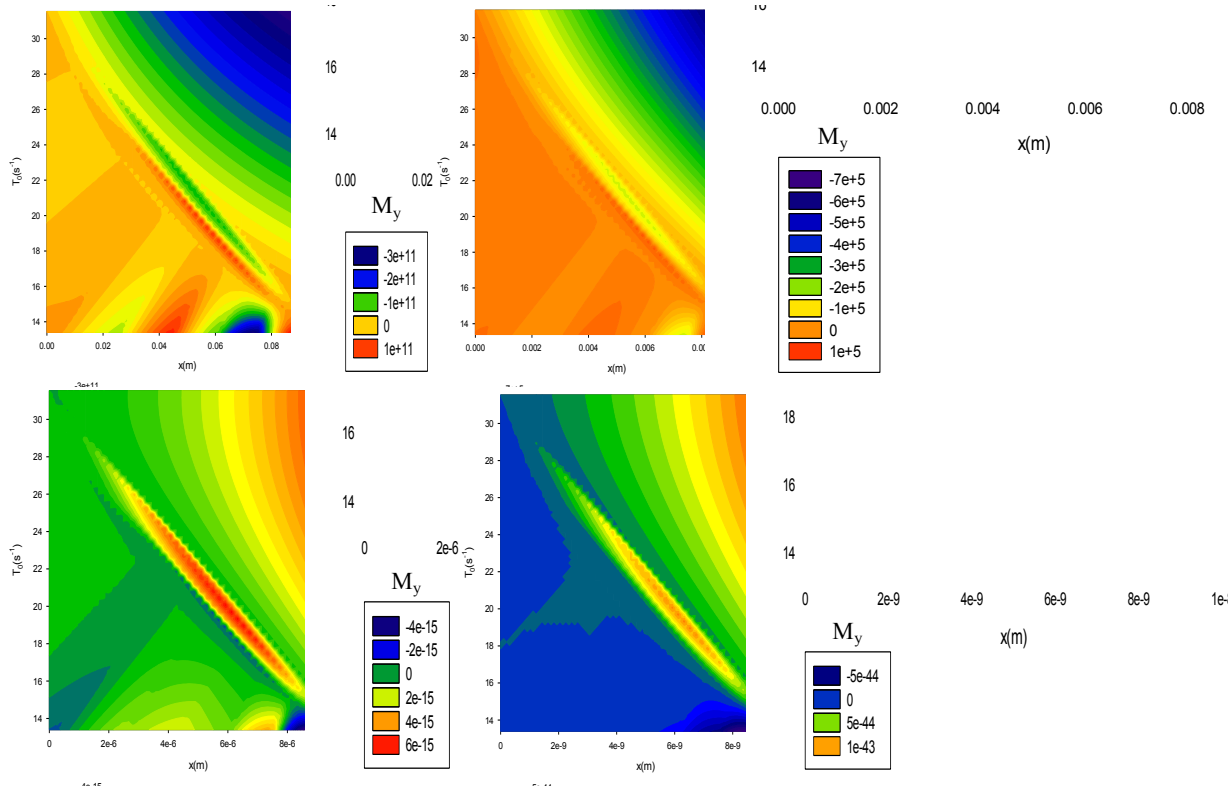

Fig. 11. Density maps of transverse magnetization as a function of location, x (at different value ranges) and T_0 for kidney at 1.5T based on tables 6 – 9.

4 Conclusion

In this contribution, we have developed the Bloch NMR flow equation into Bessel differential equation in terms of relevant NMR/MRI flow parameters. The solutions of the Bessel equation in terms of the MRI parameters make this method unique and significantly useful for computational and experimental studies of tissue NMR/MRI. The goal is to apply the abundantly available Bessel functions and properties for re-solving the difficulties usually encountered in previous and current MRI studies.

The procedure for using the traditional pulsed NMR is strictly followed [10]: (i) a conventional spin echo NMR experimental set-up is used; (ii) the 90^o pulse initiates

the measurement; (iii) the magnetic field gradient pulse with a magnitude and direction described by G and of duration δ is applied; (iv) the 180^{o} pulse is applied; (v) the magnetic field gradient pulse is repeated; (vi) the spin echo signal is received at a time 2τ *;* and (vii) a small, steady field gradient exists at all times during the experiment which often has negligible effect, but if necessary a correction factor can be added to account for this gradient.

Basically, the measurement of restricted flow may be carried out by varying *(a)* the magnitude G of the pulsed gradient, *(b)* the duration δ of the pulsed gradient, *(c)* the length of time τ between gradient pulses, or *(d)* any combination of these. These variations can be achieved conveniently by solving equation (5) which is Bessel equation of order β with parameter θ. Specifically table 1 and figures (2-9) show the computational analyses of skeletal muscle, heart muscle, liver, kidney, spleen, fatty tissue, gray brain matter and white brain matter based on the solution of Bessel equation. The peak signals are shown for each tissue at different geometrical ranges. In tables (2-9) and figures (10-11), the density maps of transverse magnetization as a function of location, x (at different value ranges) and T_0 for liver and kidney at 1.5T are presented. This demonstrates the ease with which 3D image reconstruction can be achieved.

The tables show the influence of time τ on the NMR signal. For example in human kidney at 1.5T, when the relaxations times are mapped to locations x within the range 0 to 10×10^{-9}m as shown in table 9, as time τ increases, the transverse magnetization decreases. Generally it is observed that the influence of time τ on the NMR signal depends on the specific tissue being imaged and the value of x. The advantage of this is that computational MRI experiments can be carried out more accurately using Bessel functions and properties.

References

1. Brix G., Kolem H., Nitz W.R., Bock M., Huppertz A., Zech C.J., Dietrich O. Basics of Magnetic Resonance Imaging and Magnetic Resonance Spectroscopy. Springer Berlin Heidelberg, 2008.
2. Dawson, J. and Lauterbur, P.C. (2008) Magnetic resonance imaging. *Scholarpedia* 3(7):3381: available at http://www.scholarpedia.org/article/Magnetic_resonance_imaging

3. O.B. Awojoyogbe, M. Dada: Mathematical Design of a Magnetic Resonance Imaging Sequence Based on Bloch NMR Flow Equations and Bessel Functions. Chin J Magn Reson Imaging, 2013; 4(5): 379-386.
4. O.M. Dada, O.B. Awojoyogbe O. A. Adesola and K. Boubaker: Magnetic Resonance Imaging Derived Flow Parameters for the Analysis of Cardiovascular Diseases and Drug Development, Magnetic Resonance Insights 2013; 6: 83–93 (available from http://www.la-press.com).
5. Awojoyogbe O.B. and Boubaker K. A. Solution to Bloch NMR flow equations for the analysis of hemodynamic functions of blood flow system using m-Boubaker polynomials. Curr Appl Phys 2008; 9(1): 271-83.
6. Awojoyogbe O.B. A quantum mechanical model of the Bloch NMR flow equations for electron dynamics in fluids at the molecular level. Physica Scripta 2007; 75: 788-794.
7. Wylie C.R. and Barrett C.L. (1982). Advanced Engineering Mathematics. McGraw-Hill, Tokyo, Japan. Pp 586 – 587.
8. Spiegel MR. Schaum's Outline Series of Theory and Problems of Advanced Mathematics. McGraw-Hill: Singapore 1983.
9. Price WS. Pulsed Field Gradient Nuclear Magnetic Resonance as a Tool for Studying Translational Diffusion: Part I. Basic Theory. Concepts Magn. Reson. 1997; 9: 299-336.
10. Tanner J.E. Magnetic Resonance in Colloid and Interface Science: ACS Symp. Ser. 1976; No. 34 p 16.